Mass-conservation sets excitable pulse collisions to be spatiotemporal organizing centers

Arik Yochelis,[1,2] Carsten Beta,[3] and Nir Gov[4]

[1]*Department of Solar Energy and Environmental Physics, Blaustein Institutes for Desert Research (BIDR), Ben-Gurion University of the Negev, Sede Boqer Campus, Midreshet Ben-Gurion 8499000, Israel*

[2]*Department of Physics, Ben-Gurion University of the Negev, Be'er Sheva 8410501, Israel*

[3]*Institute of Physics and Astronomy, University of Potsdam, 14476 Potsdam, Germany*

[4]*Department of Chemical and Biological Physics, Weizmann Institute of Science, Rehovot 76100, Israel*

(Received July 15, 2019)

Outcomes of propagating pulse collisions are of fundamental importance in many fields, ranging from physiology to industrial devices. Pulses are traditionally classified as solitons if upon collision they behave as particles, or excitable-pulses if they annihilate each other. Collisions in a non-equilibrium system with mass conservation, a common property of natural systems, exhibit rich dynamics that range from soliton-like to annihilation, and even nucleation of new pulses post-collision. Mass-conservation is shown to be a key ingredient for this behavior to occur robustly over a wide range of parameters. As such, collisions can be considered as organizing centers, for example, in intracellular actin waves.

Study of propagating solitary pulses is cross-disciplinary and also extends beyond basic science due to their important applications in biological, chemical and physical systems [1]. Although observation of a solitary wave dates back to John S. Russell (1834), only after the work of Zabusky and Kruskal [2] were solitary waves distinguished by their collision properties [3]: *solitons* if after collision of two pulses, two pulses emerge (particle-like identity) and *dissipative solitons* or *excitable pulses* if they are annihilated.

Solitons are often being discussed in the context of conservative media, which mathematically means exploiting the integrable nature of the governing model equations [4]. On the other hand, excitable pulses often arise in reaction–diffusion (RD) type systems that are used as model equations to scrutinize chemical and biological patterns. These RD equations contain far-from-equilibrium auto-catalytic or enzymatic terms that are typical in non-conserved media [5, 6]. Moreover, owing to their general phenomenology, they also emerge over a wide range of scales, e.g., in surface reactions [7], gas discharge plasmas [8], intracellular actin dynamics [9], cardiac rhythms [10] and neuroscience [11].

Although collisions of solitons may involve high spatiotemporal complexity, the outcome of two colliding solitons remains unchanged (i.e., elastic particle-like dynamics) [12, 13]. On the other hand, the annihilation of excitable pulses after the collision is recognized as paramount for electrophysiological function, i.e. it would be impossible to maintain directionality, and thus rhythmic behavior, under the reflection of action potentials [14]. Therefore, the distinction between solitons and excitable pulses is important for applications. However, this distinction is blurred upon identification of soliton-like behavior in RD-type media [7, 13, 15], along with theoretical studies [16] that demonstrate the existence of soliton-like behavior in far-from-equilibrium systems.

Collisions are essentially spatially localized in space and can be, therefore, considered as focal perturbations. Beyond annihilation or reflection, such perturbations can give rise to more complex dynamics. For example, it has been shown that in excitable media, *single* focal perturbations may generate distinct multiple-integer pulse trains [17]. Consequently, we may ask if collisions can act as organizing centers for persistent spatiotemporal emergence of excitable waves?

In this Letter, we show distinct aspects of excitable pulse collisions, by studying a mass-conserved RD framework. Our motivation stems from the observations of complex behavior of intracellular waves [18–20]. Thus, we employed and analyzed without a loss of generality, a reduced version of a system that has been formulated for actin polymerization in circular dorsal ruffles [20]. The dynamics is rich, exhibiting regimes of annihilation, reflection and nucleation of additional pulses after a collision. Specifically we emphasize that the mass-conserved RD framework is capable of supporting solitary pulses that have both soliton-like and excitable collision characteristics. The appearance of such pulses is robust over a wide range of parameters and does not require proximity to an oscillatory onset [21] nor non-local interactions [22]. Implications to intracellular and chemical phenomena that exhibit mass-conserved RD characteristics are discussed at the end.

Mass-conserved RD model– We start with an RD model that was formulated to study front dynamics of circular dorsal ruffles (CDR) [20], which are waves of actin polymerization that propagate on the dorsal side of the cell membrane. We reduce this model to a simpler version that includes filamentous actin and an inhibitor of actin polymerization. The three species in this minimal version are: (*i*) Polymerized actin filaments (F-actin) that are organized in a network (dendritic-like) mor-

phology, $N(x,t)$, (*ii*) Actin monomers (G-actin) $S(x,t)$, and (*iii*) an actin polymerization inhibitor, $I(x,t)$. In accordance with the CDR model, we employ actin mass-conservation: $\int_\Omega \{N(x)+S(x)\}\,\mathrm{d}x = A$, where $x \in \Omega$ is the spatial domain size and A is constant. In comparison with the CDR model, we have excluded from the current model the additional reservoirs of polymerized actin in the cortex and in stress fibers. Adding them complicates the analysis and does not qualitatively change the nature of the solitary pulses, which are the focus of this study.

The continuum model in its dimensionless form reads [20]:

$$\frac{\partial N}{\partial t} = \frac{N^2 S}{1+I} - N + D_\mathrm{N}\frac{\partial^2 N}{\partial x^2}, \tag{1a}$$

$$\frac{\partial S}{\partial t} = -\frac{N^2 S}{1+I} + N + \frac{\partial^2 S}{\partial x^2}, \tag{1b}$$

$$\frac{\partial I}{\partial t} = k_\mathrm{N} N - k_\mathrm{I} I + D_\mathrm{I}\frac{\partial^2 I}{\partial x^2}, \tag{1c}$$

Eqs. 1a,1b describe the auto-catalytic polymerization process, converting monomers to filaments, which is inhibited by the presence of I, and with a constant rate of depolymerization. Eq. 1c describes the recruitment of the inhibitor to the filamentous actin.

The hierarchy of diffusion coefficients, along the membrane, is such that the monomers diffuse the fastest, while the effective diffusion of polymerized actin is slower and mostly occurs by the polymerization activity. The inhibitor diffuses the slowest as it is adsorbed to the membrane [20]: $D_\mathrm{I} \ll D_\mathrm{N} < 1$. In fact, D_I is not essential for what follows, but we keep it as it makes the comparison to the FitzHugh-Nagumo (FHN) model [21] transparent. In addition, we chose $k_\mathrm{I} < k_\mathrm{N}$ [20], but this is not essential. We employ Neumann (no-flux) boundary conditions (BC), while similar results (not surprisingly) are obtained with periodic BC.

Linear stability analysis of uniform solutions– Our interest is in pulses, a situation that requires linear stability of a uniform solution [4]. Eqs. 1 admit three uniform solutions $\mathbf{P} \equiv (N,S,I)^T$:

$$\mathbf{P}_0 = (0,A,0)^T, \quad \mathbf{P}_\pm = (N_\pm, A-N_\pm, {}^{k_\mathrm{N}}\!/_{k_\mathrm{I}} N_\pm)^T,$$

where, $N_\pm = \frac{1}{2}\left[A - {}^{k_\mathrm{N}}\!/_{k_\mathrm{I}} \pm \sqrt{(A-{}^{k_\mathrm{N}}\!/_{k_\mathrm{I}})^2 - 4}\right]$ and superscript T stands for transpose. Beyond the saddle–node (fold) bifurcation at $A > A_c = {}^{k_\mathrm{N}}\!/_{k_\mathrm{I}} + 2$ (Fig. 1(a), top panel), the solutions $\mathbf{P}_\pm$ appear: $\mathbf{P}_-$ is unstable by definition, while linear stability analysis of $\mathbf{P}_+$ to uniform perturbations shows that it is also unstable to Hopf oscillations, already from the saddle–node bifurcation point.

Next, we check linear stability of $\mathbf{P}_{0,+}$ to nonuniform perturbations on an infinite domain [6],

$$\mathbf{P} - \mathbf{P}_{0,+} \propto e^{\sigma t + iqx} + \text{complex conjugate},$$

where, σ is the growth rate of perturbations that are characterized by wavenumbers q. We find that solution $\mathbf{P}_0$ continues to be linearly stable and does not lie in a proximity to any linear oscillatory instability since all parameters are positive, with dispersion relations:

$$\sigma_N = -1 - D_\mathrm{N} q^2, \quad \sigma_S = -q^2, \quad \sigma_I = -k_\mathrm{I} - D_\mathrm{I} q^2. \tag{2}$$

While the solution $\mathbf{P}_+$ was found to be unstable to uniform perturbations, we find that it is unstable also to traveling waves, i.e., non-vanishing imaginary part of its eigenvalue σ_+. However, these traveling waves are beyond the scope of our interest here and therefore, not shown.

Notably, the signature of mass-conservation is reflected in the persistence of the neutral mode $\sigma(q=0) = 0$ for the S field (Eq. 2), which indicates a respective mass exchange between N and S. This property is absent in the typical RD system without mass conservation, e.g., FHN [21], and in what follows, we show that it plays an essential role during the collision of two counter propagating pulses, as shown in Fig. 1.

Spatial dynamics and the collision zone– As has been shown by Argentina *et al.* [21], information about the possible behavior after a collision between pulses can be deduced by looking at the geometric structure of the collision zone, i.e., by understanding the instability of coexisted symmetric steady–state solution to which the propagating pulses attempt to emerge at the collision, a.k.a *nucleation droplet*. Such spatially localized states are associated with an intersection of two-dimensional stable and unstable manifolds in space [4, 23], meaning that pulse solutions connect asymptotically to $\mathbf{P}_0$ at $x \to \pm\infty$.

To identify the geometric structure of the nucleation droplet, we rewrite (1) as a set of ordinary differential equations in a co-moving frame $\xi = x - ct$, where c is the pulse propagation speed:

$$\frac{\mathrm{d}N}{\mathrm{d}\xi} = u, \ \frac{\mathrm{d}S}{\mathrm{d}\xi} = v, \ \frac{\mathrm{d}I}{\mathrm{d}\xi} = w, \ \frac{\mathrm{d}u}{\mathrm{d}\xi} = \frac{N - \frac{N^2 S}{1+I} - cu}{D_\mathrm{N}},$$
$$\frac{\mathrm{d}v}{\mathrm{d}\xi} = \frac{N^2 S}{1+I} - N - cv, \ \frac{\mathrm{d}w}{\mathrm{d}\xi} = \frac{k_\mathrm{I} I - k_\mathrm{N} N - cw}{D_\mathrm{I}}, \tag{3}$$

and perform linear (asymptotic) analysis in space [4]:

$$\mathbf{P} - \mathbf{P}_0 \propto e^{\lambda\xi} + \text{complex conjugate}.$$

The resulting spatial eigenvalues are: $\lambda_0 = 0$, $\lambda_\mathrm{c} = -c$, $\lambda_{\pm\mathrm{N}} = \pm D_\mathrm{N}^{-1}$, $\lambda_{\pm\mathrm{I}} = (2D_\mathrm{I})^{-1}\left[-c \pm \sqrt{c^2 + 4D_\mathrm{I} k_\mathrm{I}}\right]$.

Inspection of the eigenvalues shows two distinct feature as compared to the FHN system: (*i*) The eigenvalues are all real so that the hyperbolic intersection at $\mathbf{P}_0$ results in monotonic tails of the pulses (Fig. 1(vi), $t = 100$), unlike in the FHN case, where the tails are oscillatory due to complex eigenvalues (which also indicates proximity to a Hopf onset in the FHN case), (*ii*) in

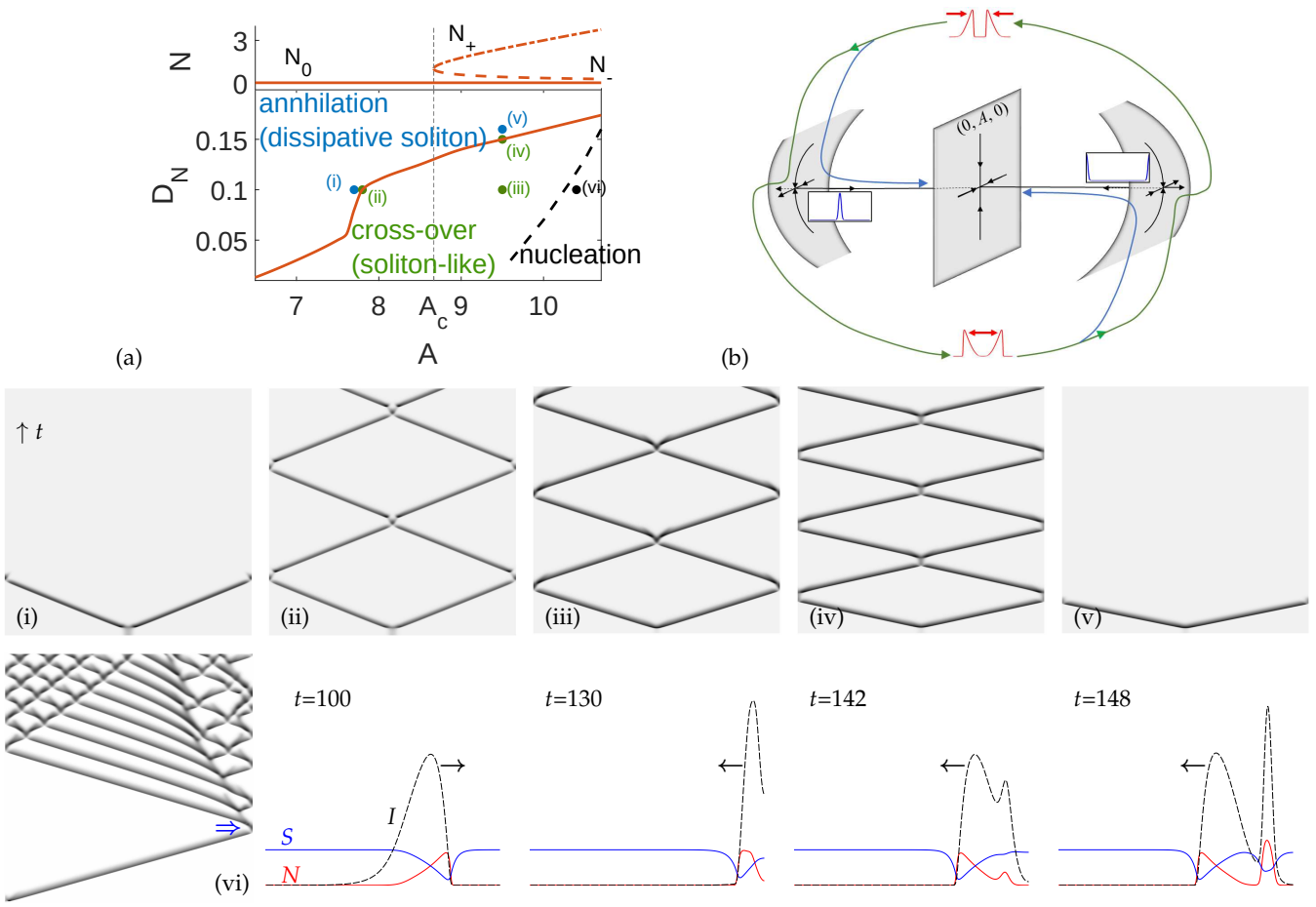

FIG. 1: (Color online) (a) Bifurcation diagram for uniform states (top panel), where solid line indicates linear stability and otherwise unstable to waves. Dashed line indicates instability to uniform perturbations, whereas dashed-dotted line indicates instability to uniform Hopf and A_c marks the location of the saddle node above which three solutions coexist. Parameter plane (bottom panel) reflecting distinct behaviors after collision of two excitable pulses and also the nucleation region (below dashed line). (b) Schematic representation of a simplified geometrical configuration for the collision process that is based on [21], see also text for details. The gray shaded regions represent the essential directions of manifolds, which are of much higher dimensional. The middle region is related to the fixed point $\mathbf{P}_0$ while the right-left domains to the nucleation droplet, as shown in the insets, respectively. The top-bottom insets, show propagating pulses and soliton-like (outer path) or annihilation (inner path) behavior. (i)-(vi) Space–time plots computed by direct numerical integration of (1), with dark color indicating larger amplitude of N, domain size $x \in [0, 100]$, time interval $t \in [0, 400]$, and Neumann (no-flux) boundary conditions, where: (i) $A = 7.7$, $D_{\rm N} = 0.1$, (ii) $A = 7.8$, $D_{\rm N} = 0.1$, (iii) $A = 9.5$, $D_{\rm N} = 0.1$, (iv) $A = 9.5$, $D_{\rm N} = 0.15$, (v) $A = 9.5$, $D_{\rm N} = 0.16$, (vi) $A = 10.4$, $D_{\rm N} = 0.1$. In (i)-(v) the initial conditions are linear perturbations of an unstable steady–state solutions at respective values (e.g., Fig. 2). The spatial profiles right to (vi), show explicitly nucleation of new excitation after the first collision (see arrow in space-time plot) at indicated times, where dark arrows indicate directions of motion and $x \in [50, 100]$. Other parameters: $D_{\rm I} = 0.001$, $k_N = 2$, $k_N = 0.3$, $A_c = 8\,2/3$.

addition to the 2D stable and unstable manifolds (as for FHN), an additional 2D manifold coexists, and specifically it becomes neutral at $c = 0$, where $\lambda_0 = \lambda_{\rm c} = 0$. The eigenvalue $\lambda_0 = 0$ is a signature of the mass conservation while $c = 0$ implies a spatially symmetric (static) pulse solution. In fact, the 2D manifold that is associated with $\lambda_{\pm {\rm I}}$ is not essential and all the results persist also for $D_{\rm I} = 0$, for which $\lambda_{\rm I} = k_{\rm I}/c$. Indeed, a computation for $D_{\rm I} = 0$, shows that both the nucleation droplet and the eigenfunction are essentially identical, see in Fig. 2. In other words, the intersection with 2D neutral manifold which arises from mass-conservation, i.e., the constraint that it imposes on the 2D manifold of $\lambda_{\pm {\rm N}}$, adds distinct features as compared to non-conserved RD system.

Numerical analysis and interpretation– After identifying

the necessary conditions for the nucleation droplet, we turn to numerical verification by solving Eqs. 3 as a standard boundary value problem with $c = 0$. Indeed, we obtain a spatially symmetric stationary pulse solution that asymptotes to $\mathbf{P}_0$ as $x \to \pm\infty$, as shown in Fig. 2(a). Solving next the eigenvalue problem for the obtained pulse solution, we find that it is indeed linearly unstable. However, we also find that the critical information lies in the neutral eigenvalue, for which the associated eigenfunction is localized, as shown in Fig. 2(b). Notably, we get the same nucleation droplet and localized eigenfunction in the absence of diffusion of the inhibitor, for $D_{\mathrm{I}} = 0$. In the absence of mass conservation, this type of neutral eigenvalue and localized eigenfunction are absent. In the FHN model the nucleation droplet goes through a Andronov-Hopf instability [21], and is oscillatory.

The form of the localized eigenfunction (Fig. 2(b)) implies a splitting process of the nucleation droplet, and the initiation of soliton-like behavior over a wide range of parameters. To verify both nucleation and post-collision behavior, we use the nucleation droplet as an initial condition for direct numerical integration of Eqs. 1. The parameters for the calculations are indicated by the points (i)-(vi) in Fig. 1(a), while the space-time plots are shown with their respective numeral label. We chose examples from regimes where two colliding pulses (i,v) annihilate (dissipative excitable solitons) or (ii-iv) persist (soliton-like) upon collision.

However, mass-conservation apparently, holds another post-collision feature, which is related to the spontaneous emergence of a new symmetric pulse at the tail

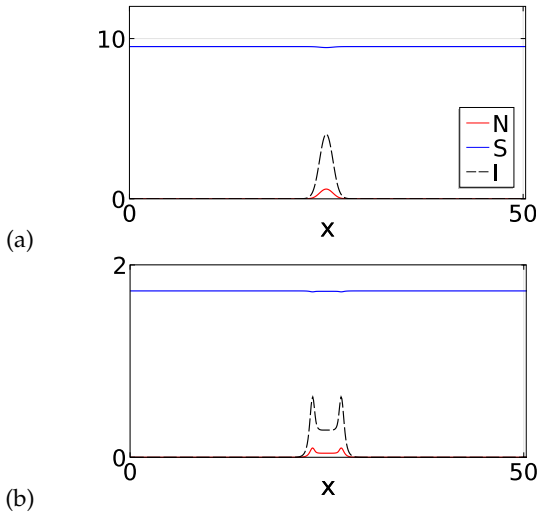

FIG. 2: (Color online) (a) A typical unstable steady-state solution to (1) computed numerically via boundary value problem at $A = 9.5$, $D_{\mathrm{N}} = 0.1$, i.e., point (iii) in Fig. 1. (b) Eigenfunction of steady–state solution (a) that corresponds to the neutral eigenvalue.

of each pulse after the collision takes place. The behavior is marked as *nucleation* region in Fig. 1(a). Panel (vi) shows a space-time plot at which these nucleation processes are formed giving rise to a persistent wavy pattern. The profiles on the left of panel (vi) show a single boundary-collision event (see double arrow in (vi)) after which a new symmetric pulse emerges. Formation of this new pulse is related to mass-conservation. After the collision, the lagging inhibitor (after the leading pulse front, N) is concentrated in space to high values ($t = 130$). This over-shoot in I creates a steep decrease also at the back of the pulse, much faster than the steady-state exponential decay (see $t = 100$, before the reflection). The depolymerized mass of N is conserved and converted into a high density of monomers S, which provide the substrate for the nucleation of a new (almost symmetric) pulse ($t = 142$). This nucleation can then either decay (the soliton-like behavior as in (ii)-(iv)) or grow ((vi), $t = 148$), and then split into two new counter-propagating pulses, which subsequently generate the pattern shown in (vi). Naturally, a similar nucleation mechanism does not occur in RD media without mass conservation since the deformation of the pulses is not constrained, and the nucleation droplet is oscillatory, which can at most give rise to multiple oscillating waves upon pulse collisions [21].

To summarize the analysis, we follow for convenience the schematic (and in our case also over simplified) geometrical representation by Argentina *et al.* [21]. In Figure 1(b), we show the essential manifolds for pulses that collide either at the middle of the domain or at the boundaries, where the main difference as compared to RD media [21], is the center manifold for the nucleation droplet, see the most left and right profiles.

Discussion– Mass conservation constraints are particularly important in enclosed systems, such as biological cells, and indeed have recently attracted increasing attention in the context of reaction-diffusion modeling of intracellular patterns in general [24]. We have shown in this study that RD media with mass conservation can support rich spatiotemporal dynamics following pulse collisions: annihilation, reflection, and "birth" of new pulses after reflection. Due to mass-conservation, this behavior is robustly observed over a wide range of parameters. No special conditioning, such as proximity to a bifurcation point or non-locality, is required, in contrast to RD-type systems without explicit mass conservation [25].

The phenomena are specifically relevant to actin waves that occur in a wide range of cell types [26], including *Dictyostelium* cells [18, 27], neutrophils [28], and fish keratocytes [29]. Although still under debate, their role has been associated with essential cellular functions, such as polarity formation, motility, and phagocytosis. Sustained wave activity may thus become a key requirement for proper cell function. Soliton-like

collisions and pulse nucleation that robustly emerge in a mass-conserved system can be seen as a strategy to maintain prolonged wave activity without depending on local heterogeneities or actively introduced nucleation events. In this regime, waves persist and replicate, in contrast to a "classical" excitable media, where pulses mutually annihilate upon collision or decay at the boundaries. Moreover, we may also envision that cells control their level of intracellular wave activity by gradually shifting between regimes of pulse annihilation and soliton-like behavior.

We therefore, exemplified our findings using a model of intracellular actin polymerization that describes the dynamics of circular wave patterns at the dorsal membrane of adherent cells [20]. Thus, the effects of mass conservation on pulse collision dynamics presented here will stimulate future progress in the modeling of actin waves and will advance our understanding of intracellular wave patterns in general. Moreover, they will also impact studies of non-biological media, such as catalytic surface reactions and electrochemical systems that exhibit solitary waves [7, 30], where surface coverage often obeys mass conservation [31].

[1] N. Akhmediev and A. Ankiewicz, *Dissipative Solitons: From Optics to Biology and Medicine*, Vol. 751 (Springer Science & Business Media, 2008); H.-G. Purwins, H. Bödeker, and S. Amiranashvili, Advances in Physics **59**, 485 (2010).

[2] N. J. Zabusky and M. D. Kruskal, Physical Review Letters **15**, 240 (1965).

[3] A. C. Scott, F. Chu, and D. W. McLaughlin, Proceedings of the IEEE **61**, 1443 (1973); A. C. Scott, Rev. Mod. Phys. **47**, 487 (1975).

[4] E. Knobloch, Annu. Rev. Condens. Matter Phys. **6**, 325 (2015).

[5] E. Meron, Physics Reports **218**, 1 (1992).

[6] M. C. Cross and P. C. Hohenberg, Rev. Mod. Phys. **65**, 851 (1993).

[7] H. Rotermund, S. Jakubith, A. von Oertzen, and G. Ertl, Physical Review Letters **66**, 3083 (1991).

[8] M. Bode and H.-G. Purwins, Physica D **86**, 53 (1995).

[9] J. Allard and A. Mogilner, Curr. Opin. Cell Biol. **25**, 107 (2013).

[10] A. Karma, Annu. Rev. Condens. Matter Phys. **4**, 313 (2013).

[11] E. M. Izhikevich, *Dynamical Systems in Neuroscience* (MIT press, 2007).

[12] M. J. Ablowitz and D. E. Baldwin, Physical Review E **86**, 036305 (2012).

[13] M. Santiago-Rosanne, M. Vignes-Adler, and M. G. Velarde, Journal of Colloid and Interface Science **191**, 65 (1997).

[14] S. Alonso, M. Bär, and B. Echebarria, Reports on Progress in Physics **79**, 096601 (2016).

[15] H. Willebrand, T. Hünteler, F.-J. Niedernostheide, R. Dohmen, and H.-G. Purwins, Physical Review A **45**, 8766 (1992).

[16] H. C. Tuckwell, Science **205**, 493 (1979); J. Kosek and M. Marek, Physical Review Letters **74**, 2134 (1995); O. Mornev, O. Aslanidi, R. Aliev, and L. Chailakhyan, in *Doklady Biophysics*, Vol. 346 (New York: Consultants Bureau, c1965-c2000., 1996) pp. 21–23; O. Aslanidi and O. Mornev, Journal of Biological Physics **25**, 149 (1999); Y. Nishiura, T. Teramoto, and K.-I. Ueda, Chaos **15**, 047509 (2005); M. A. Tsyganov, V. N. Biktashev, J. Brindley, A. Holden, and G. R. Ivanitsky, Physics-Uspekhi **50**, 263 (2007); B. Lautrup, R. Appali, A. D. Jackson, and T. Heimburg, The European Physical Journal E **34**, 57 (2011); G. Young, M. Demir, H. Salman, G. B. Ermentrout, and J. E. Rubin, Physica D **395**, 24 (2019).

[17] A. Yochelis, E. Knobloch, Y. Xie, Z. Qu, and A. Garfinkel, Europhysics Letters **83**, 64005 (2008); A. Yochelis, E. Knobloch, and M. H. Köpf, Physical Review E **91**, 032924 (2015).

[18] G. Gerisch, T. Bretschneider, A. Müller-Taubenberger, E. Simmeth, M. Ecke, S. Diez, and K. Anderson, Biophys. J. **87**, 3493 (2004); T. Bretschneider, K. Anderson, M. Ecke, A. Müller-Taubenberger, B. Schroth-Diez, H. C. Ishikawa-Ankerhold, and G. Gerisch, *ibid*. **96**, 2888 (2009); M. Gerhardt, M. Ecke, M. Walz, A. Stengl, C. Beta, and G. Gerisch, J. Cell Sci. **127**, 4507 (2014).

[19] A. Yochelis, S. Ebrahim, B. Millis, R. Cui, B. Kachar, M. Naoz, and N. S. Gov, Scientific Reports **5**, 13521 (2015).

[20] E. Bernitt, H.-G. Döbereiner, N. S. Gov, and A. Yochelis, Nature Communications **8**, 15863 (2017).

[21] M. Argentina, P. Coullet, and V. Krinsky, Journal of Theoretical Biology **205**, 47 (2000).

[22] K. Krischer and A. Mikhailov, Physical Review Letters **73**, 3165 (1994); M. Mimura and S. Kawaguchi, SIAM Journal on Applied Mathematics **59**, 920 (1998); S. Coombes and M. Owen, in *Fluids and Waves: Recent Trends in Applied Analysis: Research Conference, May 11-13, 2006, the Universtiy of Memphis, Memphis, TN*, Vol. 440 (American Mathematical Soc., 2007) p. 123.

[23] A. R. Champneys, Physica D **112**, 158 (1998).

[24] J. Halatek and E. Frey, Nature Physics **14**, 507 (2018).

[25] S. Whitelam, T. Bretschneider, and N. J. Burroughs, Physical Review Letters **102**, 198103 (2009); A. Dreher, I. S. Aranson, and K. Kruse, New Journal of Physics **16**, 055007 (2014); Y. Miao, S. Bhattacharya, T. Banerjee, B. Abubaker-Sharif, Y. Long, T. Inoue, P. A. Iglesias, and P. N. Devreotes, Molecular Systems Biology **15** (2019); S. Alonso, M. Stange, and C. Beta, PloS One **13**, e0201977 (2018).

[26] C. Beta and K. Kruse, Annual Review of Condensed Matter Physics **8**, 239 (2017); N. Inagaki and H. Katsuno, Trends in Cell Biology **27**, 515 (2017).

[27] M. G. Vicker, W. Xiang, P. J. Plath, and W. Wosniok, Physica D **101**, 317 (1997).

[28] O. D. Weiner, W. A. Marganski, L. F. Wu, S. J. Altschuler, and M. W. Kirschner, PLoS Biol **5**, e221 (2007).

[29] E. L. Barnhart, K.-C. Lee, K. Keren, A. Mogilner, and J. A. Theriot, PLOS Biol **9**, e1001059 (2011).

[30] K. Krischer, N. Mazouz, and P. Grauel, Angewandte Chemie International Edition **40**, 850 (2001).

[31] Y. Y. Avital, H. Dotan, D. Klotz, D. A. Grave, A. Tsyganok, B. Gupta, S. Kolusheva, I. Visoly-Fisher, A. Rothschild, and A. Yochelis, Nature Communications **9**, 4060 (2018).